exposure on or prior to the MDRO culture collection date in cases or during the entire hospitalization in controls. The association between antibiotics and MDRO detection was assessed with χ^2 and multivariable logistic regression testing. Length of stay (LOS) was compared between groups.

Results. Of 1,181 advanced cancer patients started on palliative chemotherapy and subsequently admitted, we identified 45 cases and 135 controls (figure). Overall, median age was 75 years (range 65–95) and 48% (N = 87/180) were female. Antibiotic exposure was more likely in cases (91%, N = 41/45) vs. controls (75%, N = 101/135; P = 0.02). In regression testing adjusted for gender, LOS, and ICU stay, antibiotic use was associated with MDRO detection (OR = 3.23, 95% CI 1.1, 9.8; P = 0.04). Mean LOS was higher in those with (8.7 days, 95% CI 7.5, 10.0) vs. without (3.5 days, 95% CI 3.8, 6.1) MDRO detection (P = 0.002)

Conclusion. In older advanced cancer patients on palliative chemotherapy, antibiotic use is predictive of new MDRO detection, and patients with new MDRO detection have significantly longer LOS. These results suggest antibiotics should be used cautiously in palliative care patients in whom the burdens of MDRO detection, such as longer LOS and potential room isolation with contact precautions, may conflict with goals of care.

Table: Predictors of MDRO detection in advanced cancer patients ≥65 years on palliative chemotherapy

Predictor	OR (95% CI)	*P* value
Female gender	1.1 (0.6, 2.3)	0.71
LOS ≥ 3 days	3.5 (0.8, 16.0)	0.10
ICU stay	1.3 (0.5, 3.5)	0.63
Antibiotic use	3.2 (1.1, 9.8)	0.04

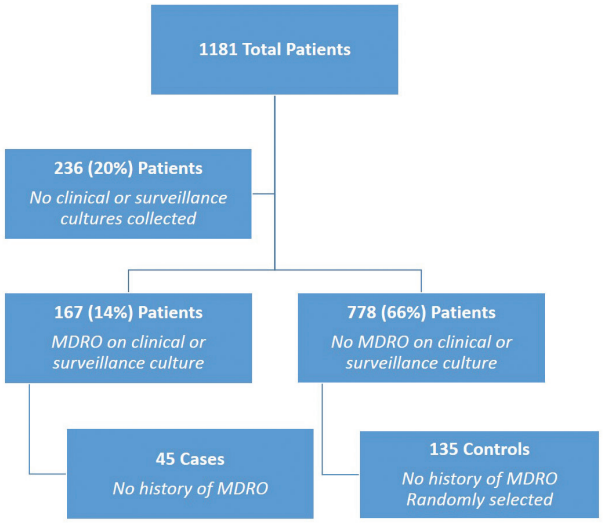

Figure 1. Study schematic of identification of cases and controls.

Disclosures. **M. Juthani-Mehta**, Iterum Therapeutics: Scientific Advisor, Consulting fee.

163. Development of an Electronic Flagging Tool for Identifying Cardiac Device Infections: Insights from the VA CART Program

Archana Asundi, MDCM[1,2]; Maggie Stanislawski, PhD[3]; Payal Mehta, MD[1]; Hillary Mull, PhD[4]; Marin Schweizer, PhD[5]; P. Michael Ho, MD, PhD[6]; Kalpana Gupta, MD, MPH[7,8] and Westyn Branch-Elliman, MD, MMSc[1,4,9], [1]VA Boston Healthcare System, West Roxbury, Massachusetts, [2]Internal Medicine, Section of Infectious Diseases, Boston University Medical Center, Boston, Massachusetts, [3]University of Colorado School of Public Health, Denver, Colorado, [4]Center for Healthcare Organization and Implementation Research, VA Boston Healthcare System, West Roxbury, Massachusetts, [5]Department of Epidemiology, University of Iowa College of Public Health, Iowa City, Iowa, [6]Seattle/Denver Center of Innovation for Veteran-Centered and Value-Driven Care, Denver, Colorado, [7]VA Boston Healthcare System, Boston, Massachusetts, [8]Boston University School of Medicine, Boston, Massachusetts, [9]Harvard Medical School, Boston, Massachusetts

Session: 46. Healthcare Epidemiology: Special Populations
Thursday, October 4, 2018: 10:30 AM

Background. Surveillance is an essential aspect of infection prevention. Despite the high morbidity and mortality associated with procedure-related Cardiac Implantable Electronic Device (CIED) infections, methods for identifying them are limited. The objective of this study was to develop an algorithm with electronic flags to facilitate detection of CIED infections in a large, multi-center cohort.

Methods. A sample of patients who underwent CIED procedures entered into the VA Clinical Assessment Reporting and Tracking Electrophysiology (CART-EP) program from FY 2007 to 2015 were included in the nested case–control study. After cohort creation, data from this review process were combined with electronic variables (e.g., microbiology orders, ICD 9/10 codes) to develop a preliminary algorithm that categorized patients as high, intermediate, or low risk of CIED infection.

Results. A total of 1,014 unique patients out of a cohort of 5,955 procedures underwent manual review. Among these cases, 59 CIED infections and 955 controls were identified. Electronic variables predictive of CIED infection included ICD 9/10 infection codes and microbiology orders (table). ICD 9/10 codes had excellent PPV for flagging infections but sensitivity was limited (47.5%, see figure). Adding microbiology order flags increased sensitivity but lowered specificity. Specificity in patients without either flag was outstanding (99%).

Conclusion. Absence of ICD 9/10 and microbiology orders is highly specific for ruling out CIED infections. The discriminatory abilities of the algorithm for intermediate probability flags (+microbiology/–ICD9/10) need improvement. In patients without ICD codes, at least microbiology orders should be used as a flag to streamline review of possible device infections. Refinement of this tool using other clinical flags may improve operating characteristics and clinical utility.

Table: Electronic flags for CIED infection

Infection flag	Infection (N = 59)	No infection (N = 955)	OR	*P*-value
CIED infection ICD 9/10	21/59 (35.6%)	1/955 (0.10%)	340	<0.001
Surgical site infection (SSI) ICD 9/10	7/59 (11.9%)	6/955 (0.63%)	18.9	<0.001
CIED infection or SSI ICD 9/10	28/59 (47.5%)	7/955 (0.73%)	64.7	<0.001
Micro order*	53/59 (89.8%)	198/955 (20.7%)	5.4	<0.001

*Blood, wound, and unclassified cultures.

Figure 1: Flow Diagram of CIED Infection Detection Tool

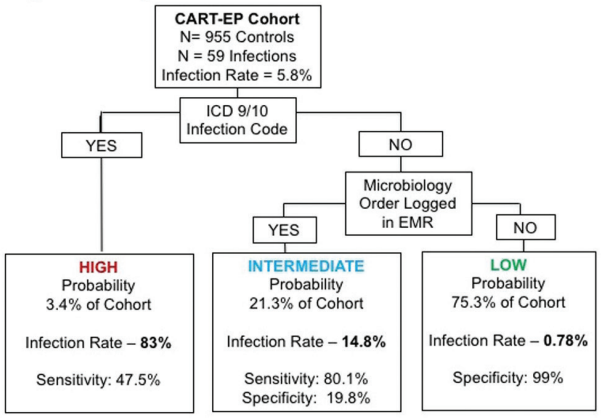

Disclosures. **W. Branch-Elliman**, Veterans' Integrated Service Network Career Development Award: Investigator, Research grant. American Heart Association: Investigator, Research grant.

164. Reporting the High-resolution Structure of the Enterococcal Ribosome: A New Template for Antibiotic Discovery

Gerwald Jogl, PhD[1]; Reza Khayat, PhD[2]; Eileen Murphy, BA[1]; Torsten Kleffmann, PhD[3]; Kavindra Singh, PhD[4]; Barbara Murray, MD[4] and Kurt Krause, MD, PhD, FIDSA[3], [1]Molecular Biology, Cell Biology and Biochemistry, Brown University, Providence, Rhode Island, [2]Chemistry and Biochemistry, City College of New York, New York, New York, [3]Biochemistry, University of Otago, Dunedin, New Zealand, [4]Internal Medicine, University of Texas McGovern Medical School at Houston, Houston, Texas

Session: 47. Science Relevant to ID
Thursday, October 4, 2018: 10:30 AM

Background. The ribosome is a rich target for antibiotic design and its structural secrets have been described at the atomic level over the past 2 decades. However, most bacterial ribosome structures come from nonpathogenic species of Archaea or thermophilic bacteria. To aid in the development of modern antibiotics against the enterococcus, we report the structure of the ribosome from *Enterococcus faecalis* at 3.5 Å resolution using cryo-electron microscopy.

Methods. *E. faecalis* strain OG1 was grown in liquid culture, collected and lysed using a French press. 70S ribosomes were purified using centrifugation through a sucrose cushion followed by column chromatography and sucrose gradient centrifugation. 70S particles were diluted in buffer and applied to a holey carbon grid and using an FEI vitrobot were flash-frozen in liquid ethane. Data were collected on an FEI Titan Krios operating at 300 kV acceleration voltage. The particles classified into 6 distinct structures based on their composition. Completed maps were utilized for structure modelling using Coot and were then refined using real space refinement within Phenix.

Results. High-quality maps of the 70S ribosome were obtained at up to 3.5 Å resolution in several distinct conformations. The 23S, 16S, and 5S RNA structures were almost completely built into maps with clear density. All but 2 ribosome proteins L25

and L33 have been placed in density. The A, P, and E sites were built into unambiguous density and found to be consistent with other bacterial structures. Notably, 1 EM density map contains an uncharged t-RNA molecule in the E site. The sites identified for current antibiotics are also well defined and interpretable. This 70S structural platform is suitable for structural analysis of antibiotic binding sites, especially for those antibiotics directed specifically against the enterococcal ribosome.

Conclusion. For the first time, the structure of the ribosome from the important human pathogen *Enterococcus faecalis* has been determined. The maps were obtained at high resolution and found to be suitable for antibiotic design. It is anticipated that the continued determination of the structures of ribosomes from pathogens will aid in the discovery of new treatments for infectious diseases.

Disclosures. **All authors:** No reported disclosures.

165. *Mycobacterium tuberculosis* Produces Molecules That Trigger Nociceptive Neurons to Activate Cough

Cody Ruhl, BS[1]; Lexy Kindt, BS, MS[1]; Haaris Khan, BS[1]; Chelsea E. Stamm, BS[1]; Breanna Pasko, BS[1]; Luis Franco, PhD[2] and Michael U. Shiloh, MD, PhD[1], [1]Internal Medicine, University of Texas Southwestern Medical Center, Dallas, Texas and [2]Center for Autophagy Research, University of Texas Southwestern Medical Center, Dallas, Texas

Session: 47. Science Relevant to ID
Thursday, October 4, 2018: 10:30 AM

Background. A hallmark symptom of active pulmonary tuberculosis vital for disease transmission is cough. The current paradigm for tuberculosis-related cough is that it results from airway damage or irritation. However, there is limited experimental data to support this theory, and whether *Mycobacterium tuberculosis* (Mtb) induces cough to facilitate its own transmission has not been explored. The cough reflex is a complex and coordinated event involving both the nervous and musculoskeletal systems initiated by particulate or chemical molecules activating nociceptive neurons, which sense pain or irritation. This activation induces a signaling cascade ultimately resulting in a cough. Respiratory nociceptive neurons innervate the airway of humans and most mammals, and thus are poised to respond to noxious molecules to help protect the lung from damage. Because Mtb is a lung pathogen, cough is a primary mechanism of Mtb transmission, and respiratory nociceptive neurons activate cough, we hypothesized that Mtb produces molecules that stimulate cough, thereby facilitating its spread from infected to uninfected individuals.

Methods. We used an *in vitro* neuronal activation bioassay to fractionate, identify, and characterize Mtb cough-inducing molecules. We also measured cough *in vivo* in response to pure Mtb-derived cough molecules and during Mtb infection using a guinea pig model.

Results. We found that an acellular organic extract of Mtb triggers and activates nociceptive neurons *in vitro* with a neuronal response that is as robust as the response to capsaicin, an established nociceptive and cough-inducing molecule. Using analytical chemistry and our neuronal bioassay, we then isolated 2 molecules produced by Mtb that activate nociceptive neurons. Both the organic Mtb extract and purified molecules alone were sufficient to induce cough in a conscious guinea pig cough model. Finally guinea pigs infected with wild-type Mtb cough much more frequently than guinea pigs infected with Mtb strains unable to produce nociceptive molecules.

Conclusion. We conclude that Mtb produces molecules that activate nociceptive neurons and induce cough. These findings have significant implications for our understanding of Mtb transmission.

Disclosures. **All authors:** No reported disclosures.

166. TGF-β Restricts T-cell IFNg Production in Pulmonary Tuberculous Granulomas

Benjamin Gern, MD[1,2,3]; Kristin Adams, PhD[1,4]; Courtney Plumlee, PhD[1]; Michael Gerner, PhD[5] and Kevin Urdahl, MD, PhD[1,2,5], [1]Center for Infectious Disease Research, Seattle, Washington, [2]Infectious Disease, Seattle Children's Hospital, Seattle, Washington, [3]Pediatrics, University of Washington, Seattle, Washington, [4]Seattle Children's Hospital, Seattle, Washington, [5]Immunology, University of Washington, Seattle, Washington

Session: 47. Science Relevant to ID
Thursday, October 4, 2018: 10:30 AM

Background. IFNg production by CD4 T cells has been thought to be critical for immunity against *Mycobacterium tuberculosis* (Mtb); however, recent studies show that IFNg-producing CD4 T cells are more effective at preventing dissemination than controlling Mtb in the lung. Because optimal control of Mtb infection requires direct interactions between CD4 T cells and Mtb-infected cells presenting cognate antigen on MHCII, we sought to determine the location of CD4 T-cell antigen recognition and IFNg production in the Mtb-infected lung.

Methods. We infected mice with an ultra-low dose (ULD) of Mtb (1–3 CFU), a model developed in our laboratory which results in well-circumscribed granulomas that recapitulate many features of human Mtb granulomas. Using immunohistochemistry and quantitative imaging, we examined their lungs 35 days later for phenotypic and spatial analysis of T-cell receptor (TCR) signaling (using IRF4) and IFNγ production. We tested the antigen specificity of these responses with an adoptive transfer of both Mtb-specific and OVA-specific control CD4 T cells into ULD Mtb-infected mice. To assess the role of TGFβ signaling on T-cell localization and function, we performed the same analysis in mice lacking the TGFβ receptor (TGFβR) on T cells.

Results. Within Mtb-infected lungs, many T cells localize near Mtb cells and undergo TCR signaling. Despite this, we found very few cells producing IFNγ within the granuloma (Figure 1). In our adoptive transfer experiment, both cell types infiltrated the granuloma. The Mtb-specific, but not OVA-specific, T cells had active TCR engagement though only a small fraction of these cells produced IFNγ, and this IFNγ was diminished near Mtb (Figure 2). Conversely, in the TGFβR conditional knockout, we found increased IFNγ production that was highest within the granuloma (Figure 3).

Conclusion. Despite ongoing TCR stimulation in T cells, IFNγ production is restricted in areas where cognate interactions are most likely to occur. TGFβ plays a critical role in mediating this effect, as T cells lacking the receptor can produce more IFNγ near infected cells. These findings help explain why IFNγ-producing T cells have limited capacity to control pulmonary Mtb infection and could guide new strategies for vaccine and immunotherapeutic development.

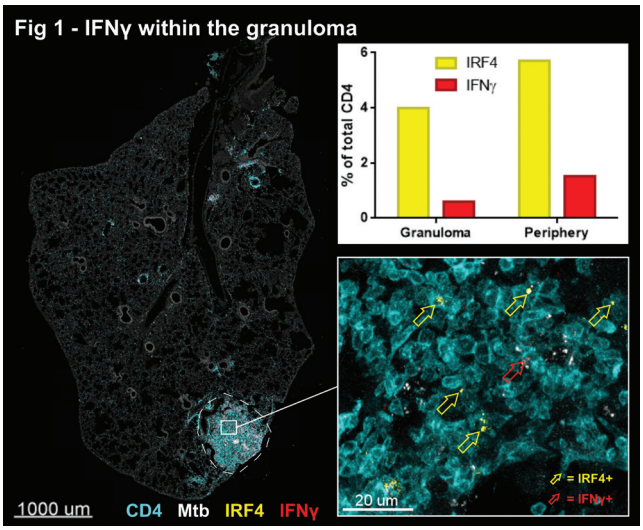

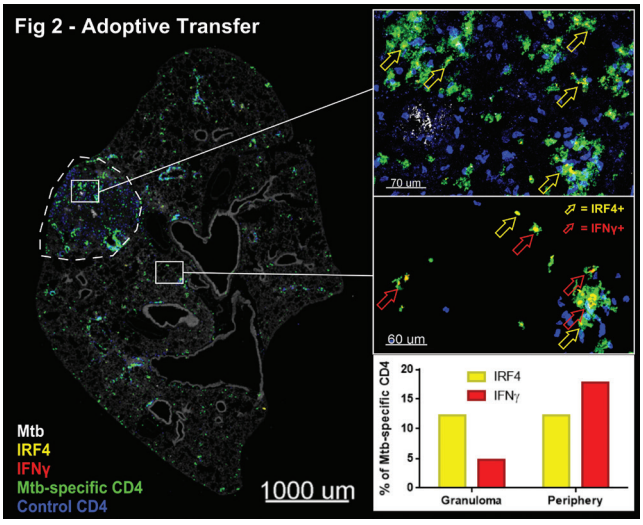

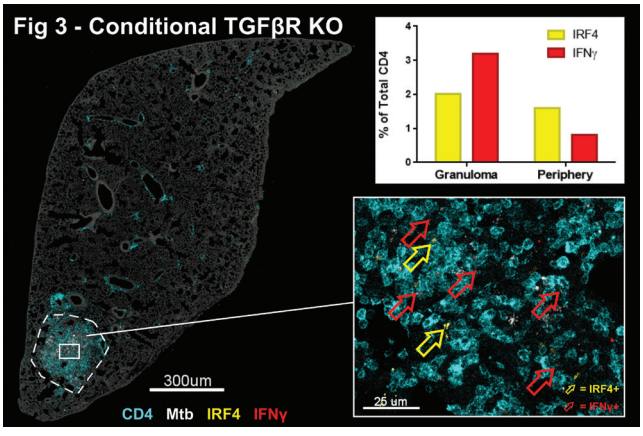

Disclosures. **All authors:** No reported disclosures.